Acta Cryst. (1971). A**27**, 399

Out-of-Zone Effects in Dynamic Electron Diffraction Intensities from Gold

BY D. F. LYNCH

Division of Chemical Physics, CSIRO, P.O. Box 160, *Clayton, Victoria* 3168, *Australia*

(*Received* 4 *August* 1970)

An investigation was made of electron diffraction from Au [111] oriented foils using the experimental method of fine-focus convergent-beam electron diffraction. The experimental data were compared directly with intensity distributions computed by multislice methods for *n*-beam diffraction from tabulated Au structure factors. Reasonable agreement could be obtained between calculation and experiment only if adequate representation was made of out-of-zone dynamic coupling. Calculations which allowed only coupling in the zone gave very poor fit with experiment and seemed only suitable for thickness estimation.

Introduction

Excellent agreement with experiment has been achieved in a number of theoretical *n*-beam dynamic electron diffraction calculations for small-unit-cell crystals composed of light atoms (Goodman & Lehmpfuhl, 1967). A variety of methods has been used including those based on the dispersion equation, the scattering matrix and the multislice formulation. It was appreciated that for heavy atoms the dynamic coupling would be greater and the calculations larger. Fisher (1968) reported *n*-beam calculations for $CuAu_3$ alloys and concluded that for many orientations 50 beams in the zone would provide quite good accuracy.

In the present study on gold [111] oriented foils the theoretical calculations have been compared with experimental results from the convergent beam electron diffraction camera. From these comparisons the errors introduced by various approximations have been evaluated. For calculations of electron diffraction from crystals of small unit cell containing only light atoms, some of the approximations that are used successfully were found to be unsuitable for gold.

Initially, thickness determination was made using the special purpose analog computer built by Johnson (1968). The high speed of this machine enabled rapid determination of the coarse features of the experimental pattern with inclusion of up to seven coupled beams. Subsequent calculations in greater detail were made by multislice methods on digital computers (CDC 3600 & 3200). It was found necessary to include up to 139 beams in these calculations in order to obtain reasonable accuracy.

Theory

The calculations made in this study make use of the Cowley–Moodie recurrence relation (Cowley & Moodie, 1957). The wave function $\Psi_m(x,y)$ at the exit face of a thin arbitrary slice of crystal is described in terms of the wave function at the exit face of the previous slice $\Psi_{m-1}(x,y)$, a propagation function $p(x,y)$ describing the phase changes due to propagation and a function $q_m(x,y)$ representing the phase changes resulting from the potential of the mth slice projected on to a two-dimensional sheet at the centre of the slice,

$$\Psi_m(x,y)=\Psi_{m-1}(x,y)*p(x,y)\,.\,q_m(x,y)\,. \qquad (1)$$

The starting point of the calculation is the wave function at the exit face of the first slice which is $q_1(x,y)$ acting on a parallel wave at normal incidence and of unit intensity. Hence it is equal to $q_1(x,y)$. It is convenient to compute with the Fourier transform of (1) which for perfect crystals can be written as

$$U_m(h,k)=[U_{m-1}(h,k)\,.\,P(h,k)]*Q_m(h,k)\,. \qquad (2)$$

Now $q_m(x,y)$, usually termed the phase grating, for finite slice thickness can be written as

$$q_m(x,y)=\exp\left\{i\sigma\int_{z_m}^{z_m+\Delta z}\varphi_m(x,y,z)\mathrm{d}z\right\}, \qquad (3)$$

where $\varphi_m(x,y,z)$ is the potential distribution in the mth slice and a relativistic σ is used

$$\sigma=\frac{2\pi m_0\lambda}{h^2}\left(1+\frac{h^2}{m_0^2c^2\lambda^2}\right)^{1/2}, \qquad (4)$$

where c is the velocity of light, m_0 is the rest mass of an electron, λ is the relativistic wavelength and h is Planck's constant. Now for a perfect crystal, φ_m is periodic in x and y; hence $q_m(x,y)$ is also. Thus the Fourier transform of $q_m(x,y)$ can be written as

$$Q_m(h,k)=\int_0^b\int_0^a q_m(x,y)\exp\{2\pi i(hx+ky)\}\mathrm{d}x\mathrm{d}y\,, \qquad (5)$$

where h and k are integers denoting a particular order of reflexion. The phase grating $Q_m(h,k)$ must satisfy a unitarity test (Moodie, 1965)

$$\sum_h\sum_k Q_m(h+h',k+k')\,.\,Q_m(h,k)=1, h'=k'=0\,;$$
$$=0, \text{ all other } h',k'\,,$$

which will show to what degree it is a satisfactory non-absorbing phase object and if sufficient reflexions have

been chosen to describe the diffraction problem. In practice, for $h'=k'=0$ the phase grating is considered to be satisfactory if the result of the unitarity test is less than one by no more than 10^{-6} and for other h',k' the result differs from zero by no more than 10^{-6}. Similarly the result of a multislice calculation is considered satisfactory if at the end of the last slice the sum of intensities of the diffracted beams is not less than 0·9 (the calculation starting with unit intensity). If an insufficient number of reflexions have been chosen for the multislice operation, then the phase grating, which contains many more reflexions, rapidly absorbs intensity into the neglected weak beams.

These two properties of the Cowley–Moodie approach to the calculation of dynamic diffraction intensities are to be contrasted with eigenvalue methods of Howie & Whelan (1962) and the scattering matrix of Niehrs (1959) which are 'self-normalizing'. In these methods the calculation itself gives no indication that an insufficient number of reflexions has been taken. Some indication is given that sufficient beams have been taken if the calculation is repeated with more reflexions until no change in result is obtained. With the 'S' matrix method (Sturkey, 1962) the calculation is not necessarily self-normalizing. In practice the approximation is made that out-of-zone reflexions may be excluded; that is, those terms in the scattering matrix of the form $V_{hkl}\exp(2\pi il.z)$, as distinct from V_{hk0}, must be excluded if the solution to the scattering problem is simply $\exp\{i(M)z\}$, where M is the scattering matrix.

The Cowley–Moodie approach, however, does not indicate within the calculation the necessity to extend the calculation from one dimension in the plane of the slice (systematics approximation) to two dimensions in the plane of the slice. In multislice calculations, upper layer-line effects are always included. If the dynamic coupling is weak the effects of upper layer lines may be minimized by proper choice of slice thickness with respect to size of the array of beams chosen. The only criterion used in these respects is the degree of agreement between the calculation and the experimental results.

For computations of high energy electron diffraction patterns, $P(h,k)$ can be written as

$$P_m(h,k)=\exp\{2\pi i\Delta z_m\zeta(h,k)\}\,, \qquad (6)$$

where $\zeta(h,k)$ is the excitation error of the hk reflexion for an Ewald sphere of radius $1/\lambda$.

In practice the approximation is generally made that $q_m(x,y)$ does not vary with small changes of angle about normal incidence and hence all effects of change of angle of incidence can be taken into account in $P_m(h,k)$.

For an object periodic in the (x,y) plane a translation of the object in the (x,y) plane of a fraction of the primitive lattice vectors can be written in the reciprocal space as a phase change.

$$\mathscr{F}[q_m(x+\Delta x,y+\Delta y)]=\mathscr{F}[q_m(x,y)] \times\exp\{2\pi i(h\,.\,\Delta x+k\,.\,\Delta y)\}\,. \qquad (7)$$

It can be seen then that in the computations, the tilt of the crystal is approximated by successive shearing movements of the slices. Shearing functions are also of use in the face-centred cubic structures viewed in the [111] direction as the lattice is made up of successive identical atomic layers, each sheared by $(\frac{1}{3},\frac{1}{3})$ with respect to the previous layer.

As the magnitude of a particular $\zeta(h,k)$ approaches $1/\Delta z$ in (6) it can be seen that the phase change of this beam on propagation approaches 2π radians. This indicates that this particular reflexion will be reinforced and corresponds to an upper layer line in the reciprocal lattice due to a c spacing of Δz. The normal practice in multislice calculations is not to relate Δz to the actual c spacing in the crystal being studied. Since Δz is not related to c, the array of beams calculated must not include reflexions whose $\zeta(h,k)$ is near to or greater than $1/\Delta z$ in magnitude. If these reflexions must be included in the calculation, it is necessary to reduce the slice thickness, Δz.

In general, identical phase grating functions are used in multislice calculations; however, it is quite possible to use very thin non-identical slices through a unit cell in the crystal and thus include in the calculation information about the structure being examined in the direction of the surface normal, z. If an accurate representation of out-of-zone effects be required, the slice thickness can be much less than one unit cell. Each successive slice through the unit cell will, in general, have a different potential distribution. Thus, on performing the multislice operation through one unit cell, allowance must in general be made for

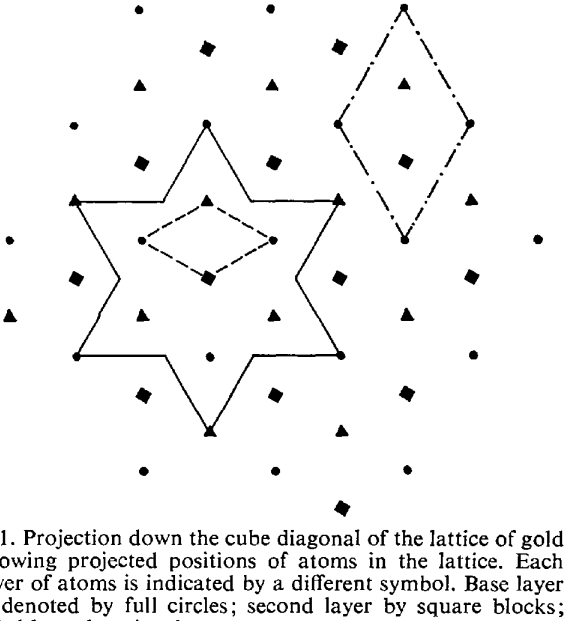

Fig. 1. Projection down the cube diagonal of the lattice of gold showing projected positions of atoms in the lattice. Each layer of atoms is indicated by a different symbol. Base layer is denoted by full circles; second layer by square blocks; third layer by triangles.

extra directions of diffraction which will have zero or near zero weight in the zone on completion of the calculation. These extra points, however, allow accurate representation of the out-of-zone reflexions. The accuracy of representation of these out-of-zone points will depend on the number of slices taken through one unit cell.

Formulation of the problem for gold

In Fig. 1 is shown the projection of one unit cell of gold onto the (111) plane of the crystal. The projection of the face-centred cubic unit cell is the star-shaped outline. The structure is made up of three identical hexagonally close-packed layers of atoms, each successive layer being translated by $(\frac{1}{3}, \frac{1}{3})$ of the primitive two-dimensional unit cell edge of one atom layer. Fig. 2(*a*) shows a region of the reciprocal lattice of gold near the origin. In this Figure is illustrated the relative positions of the [111] zone and the next two layers above the zone. In Fig. 2(*b*) is shown the [111] zone of gold. Projected onto this zone in the direction of the zone normal are the positions of the reflexions in the first and second layers above the zone.

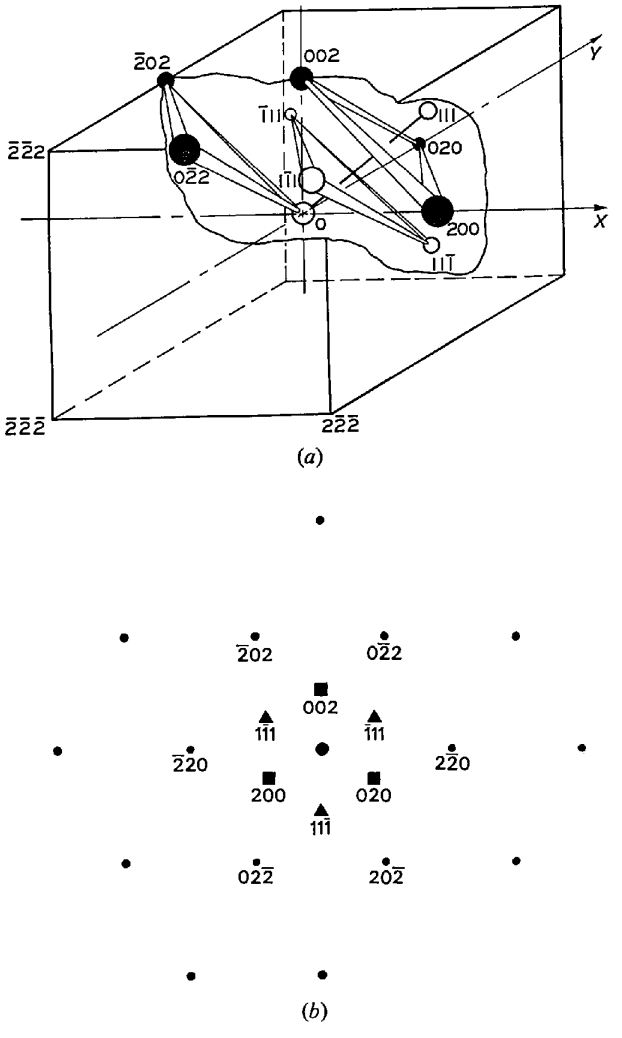

Fig. 2. (*a*) Portion of the reciprocal lattice of gold near the origin showing the [111] zone and the next two layers of reflexions. (*b*) Portion of the [111] zone of gold showing the projection onto the zone of points in the next two upper layers. Full circles are the zone points; triangles indicate projected positions of points from the first upper layer; squares denote the projected positions of the second upper layer.

The smaller of the two two-dimensional primitive cells outlined in Fig. 1 is that chosen for calculation when the full unit-cell length in the [111] direction, 7·08 Å, is chosen as the projection distance for the phase-grating calculation. Such a unit cell has the same reflexions in the zero layer as the [111] zone of the face-centred cubic gold, although it has not the same c spacing or the correct weights of reciprocal lattice points out of the [111] zone. This is the unit cell used for the calculations considering only in-zone reflexions in gold. Although there is little significant overlap of atoms in the [111] direction, in practice the 7·08 Å projection distance is too great because the effect of the pseudo upper layer line at a c spacing of 0·141 $Å^{-1}$ becomes important for 7×7 arrays of reflexions in the zone. The slice may be arbitrarily subdivided in order to reduce the pseudo c spacing and hence raise the upper layer line. In this case, three identical slices each containing one third portion of the projected potential of the full cell and of thickness 2·36 Å were sufficient to allow accurate calculations of in-zone effects.

Alternatively one may construct the phase grating for one atom layer from the larger of the primitive cells shown in Fig. 1 and perform a multislice calculation with this phase grating, at each step translating it by $(\frac{1}{3}, \frac{1}{3})$ of the primitive cell edges. By tying the slice thickness to the thickness of one atom layer (2·36 Å) a fuller representation of the complete reciprocal lattice, *i.e.* a better representation of the crystal structure, is obtained. The extra points in the zero layer of the lattice of one atom layer are reduced to zero weight every third slice when the propagation function is the identity transformation, that is when the Ewald sphere is approximated by a plane. The remaining non-zero reflexions are then identical to the phase grating obtained from projection of the full unit cell, containing the in-zone reflexions only.

If, however, the correct propagation function for the wavelength in question is included, the extra points in the calculation do not fall to zero weight every third slice but have intensities commensurate with the large excitation errors of the out-of-zone reflexions. If the angle of incidence is set such that the Ewald sphere intersects the line through one of these out-of-zone reflexions parallel to the crystal normal in the zero layer (the extra reflexion satisfied as though it were an in-zone reflexion) then every third slice the reflexion will have zero weight (Fig. 3).

For a number of atomic layers not divisible by three, there exists an incomplete layer of unit cells of gold at the surface of the crystal which means that the extra reflexions will be more intense. If in the multislicing operation one slice of atoms is sheared twice, the effect is that of a stacking fault in the crystal, *e.g.* *abc*, *ab*, *abc*, so the effect of such a defect on the calculations can be determined quite readily. Of course, if the same angular range is to be covered in the upper layer line calculation as in the equivalent zone-only calculation, three times as many reflexions must be used. Thus for multislice methods the computation time, which is proportional to the square of the number of reflexions, is increased by a factor of approximately nine in this case.

Experiment

The principal reasons for choosing gold as a specimen for this investigation were:

(i) Gold is an atom of high atomic number.

(ii) Since it is comparatively chemically inert it is improbable that thick ordered layers of gas or oxide would form on the surfaces of the crystal in the poor vacuum conditions of the electron diffraction camera. Although the effects of such layers are calculable, their presence would only further complicate the calculation of diffraction intensities.

Preparation by epitaxial growth of vacuum-deposited films on silver [111] oriented surfaces gives reasonable areas of perfect single crystal of [111] orientation. These films were prepared in a vacuum evaporation chamber at pressures of the order of 5×10^{-8} Torr and subsequently stripped from the silver substrates in a dilute nitric acid bath.

The specimens were then examined in the convergent beam diffraction camera (Cockayne, Goodman, Mills & Moodie, 1967). This camera can obtain diffraction patterns from regions of crystal of approximately 300 Å in diameter. Thus, by first examining the image of the foil in the camera, diffraction could be obtained from defect-free regions of crystal. A liquid nitrogen-cooled baffle surrounding the specimen prevented significant contamination during examination. All results reported in this investigation were obtained with an electron acceleration potential of 79 keV.

Some difficulty was experienced with specimen damage during long exposures to the electron beam. This is believed to be due to ion bombardment of the specimen resulting from small discharges and electrical breakdowns in the electron gun. In Fig. 4 is shown the effects observed in the Kossel–Mollenstedt patterns of the [111] zone axis of gold when such damage occurred. It is believed from experience with a Hitachi HU125 microscope in this laboratory that such problems can be avoided if the camera operating pressure can be reduced from 5×10^{-5} torr to less than 10^{-6} torr.

In Fig. 5 is shown a Kossel–Mollenstedt pattern near the [111] axis of a perfect region of gold crystal. By insertion of an aperture to reduce the angle of convergence in the illuminating electron beam, a convergent beam diffraction pattern of the same region or crystal can be obtained (Fig. 6), whose angle of incidence can be measured precisely by reference to the Kossel–Mollenstedt pattern. The convergent beam pattern shown is of a central beam flanked by $2\bar{2}0$ and $\bar{2}20$ reflexions. The diffracted beams are both of equal mean excitation error. The mean angle of incidence of the illuminating beam is 0·0821 radian with respect to the [111] zone axis, and the angular range represented across a disc is 0·018 radian. In Fig. 7 are shown three microphotometer traces obtained from this convergent-beam pattern along different paths. The disc in Fig. 6 which is indexed 000 displays the variation in intensity of the directly transmitted electrons which are incident on the crystal in the form of a well-defined cone having a half-angle of 0·009 radian. The discs flanking this then are a direct measure of the intensities of the $2\bar{2}0$ and $\bar{2}20$ reflexions as a function of the range of angles of incidence defined by the diameter of the 000 disc. The picture was the nearest to a systematics case observed within the large set of photographs taken. The effects of the non-systematic interaction, the horizontal bar which crosses the 000 disc, have been avoided as much as possible by taking microphotometer scans which do not intersect the bar. Hence, only a one-dimensional calculation may be necessary.

These microphotometer traces, then, are a direct measure of the variation of intensity with angle of incidence for the 000, $2\bar{2}0$ and $\bar{2}20$ reflexions. Cal-

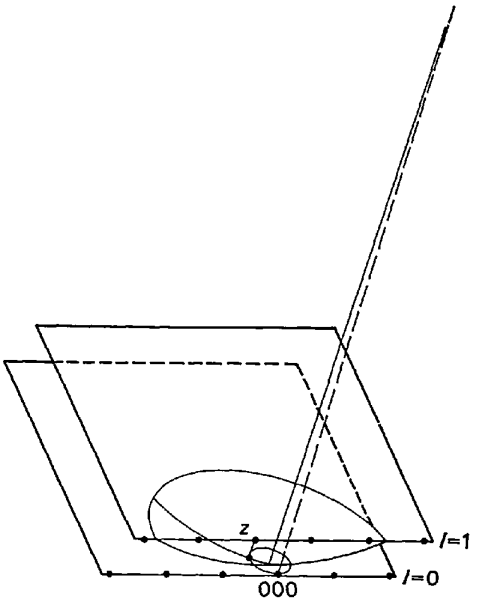

Fig. 3. Ewald sphere construction for an angle of incidence such that an out-of-zone reflexion in the first upper layer is satisfied as though it were an in-zone reflexion. z is the excitation error of a reflexion in layer $l=1$.

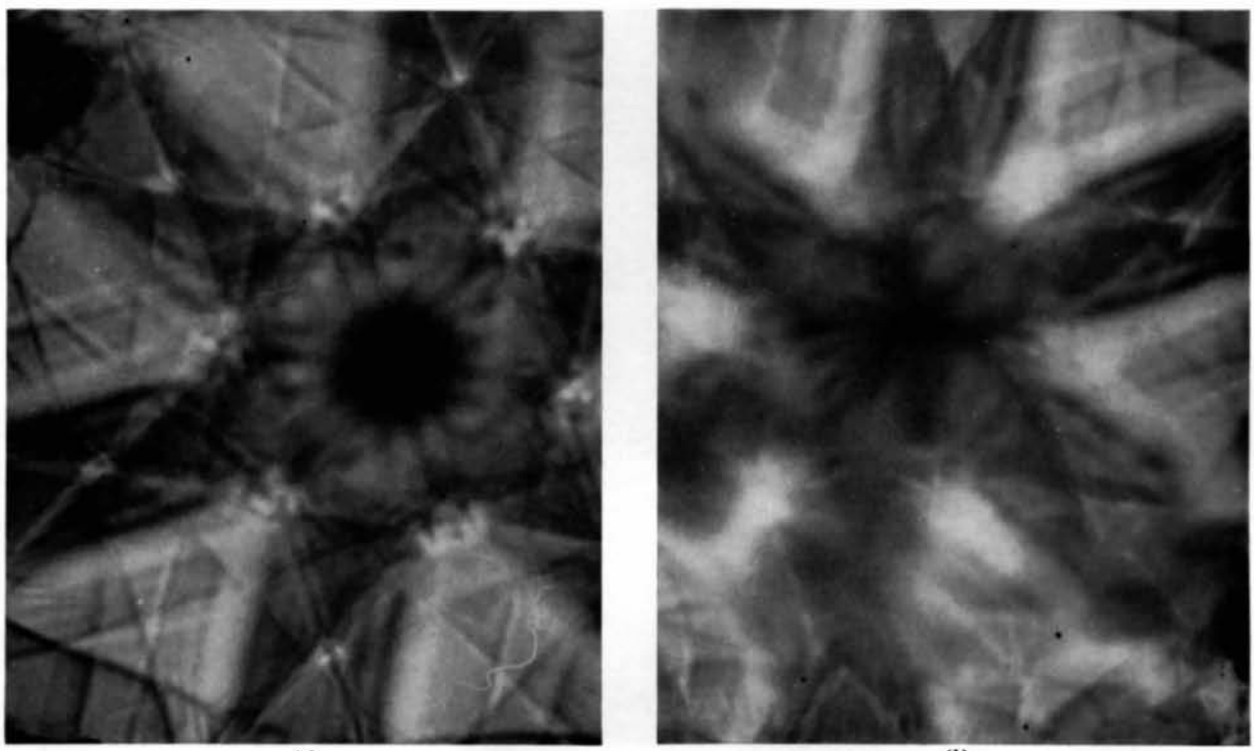

(*a*) (*b*)

Fig. 4. (*a*) Kossel–Mollenstedt pattern centred about the [111] zone of a perfect region of a gold crystal. (*b*) Kossel–Mollenstedt pattern centred about the [111] zone of a region of damaged gold crystal. This region had previously been exposed to the electron beam in the apparatus for 10 minutes.

[*To face p.* 402

Fig. 5. Kossel–Mollenstedt pattern of a perfect region of gold crystal. The pattern is centred about an angle of approximately 0·06 radian from the [111] zone axis.

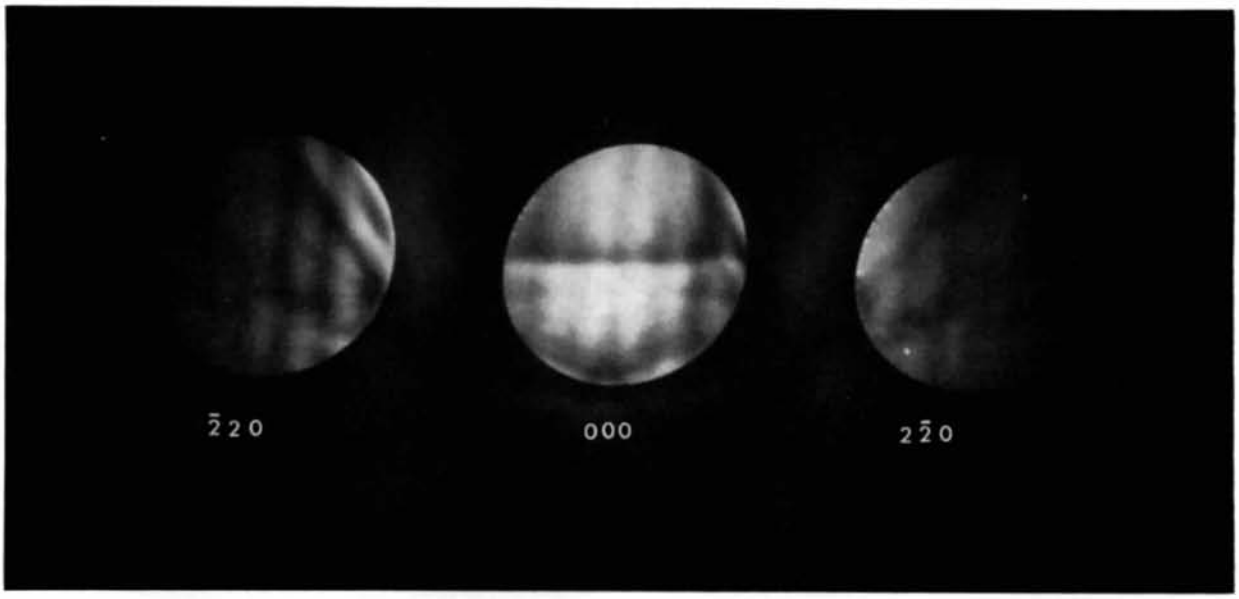

Fig. 6. A convergent beam diffraction pattern obtained by insertion of a small aperture in the electron beam which had produced the pattern shown in Fig. 5. The diffraction pattern shows a central beam flanked on each side by equally excited $\bar{2}20$ and $2\bar{2}0$ reflexions. The diameter of the central beam disc corresponds to a range of angles of incidence of 0·018 radian. The parallel bars of intensity in the central beam indicate that the picture is a near-systematics case.

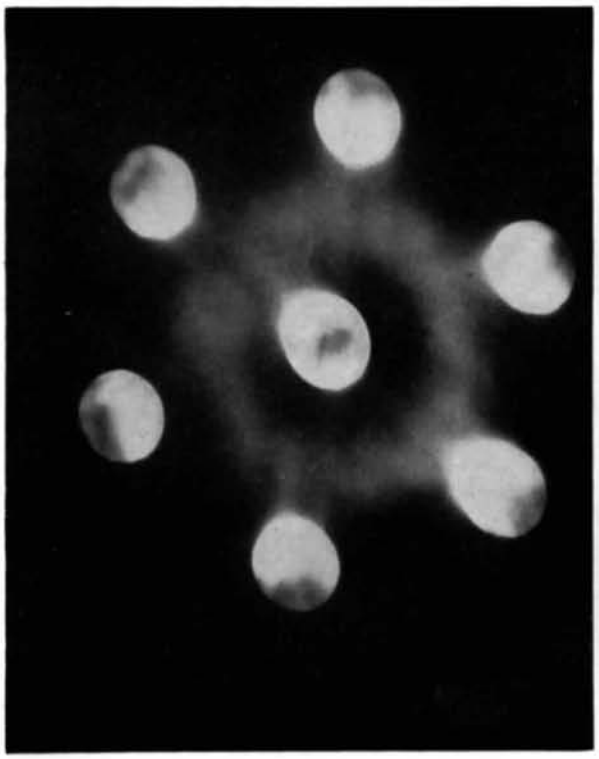

Fig. 13. Convergent beam diffraction picture, the mean angle of incidence parallel to the [111] zone axis. The region between the central beam and the 220 reflexions contains maxima in intensity in the diffuse scattering in the positions where one might find 111 and 200 reflexions. In order to bring out the region of interest some contrast enhancement has been used in the printing of the experimental picture. Also the lattice points {242} have been suppressed.

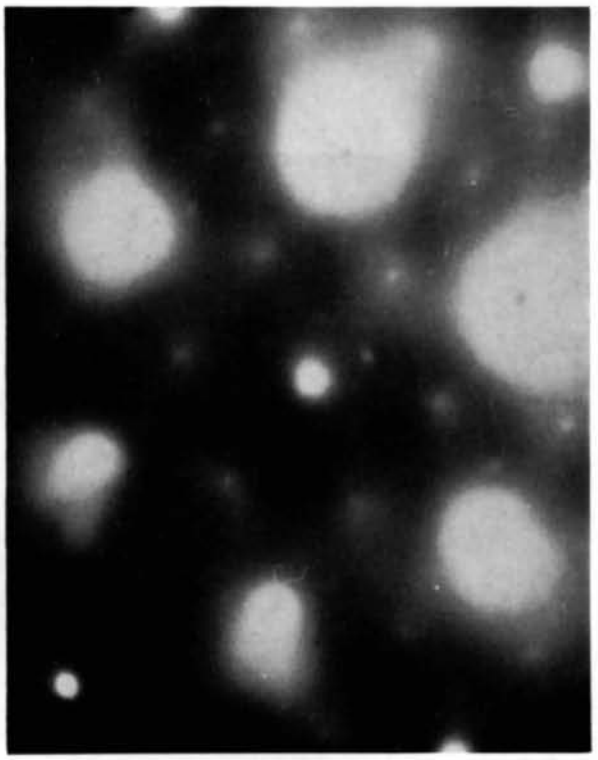

Fig. 14. Electron diffraction pattern from a [111] crystal of gold, angle of incidence parallel to the zone axis. Extra reflexions observed in the projected upper layer-line positions.

[*To face p.* 403

culations have been made in an attempt to match these experimental results.

Calculation

In the calculation, the range of angles of incidence must first be determined. This is done by comparison of experimental Kossel patterns with computed Kossel patterns (Figs. 8 & 9). Then, the crystal thickness can be determined from the analog computer. Having obtained these two parameters, angle and thickness, calculation of diffracted intensity as a function of angle of incidence at various levels of approximation can be made.

For ease of comparison of these various methods the curves of intensity of diffracted beams as a function of angle of incidence (rocking curves) have been grouped together in Fig. 10. Another method of comparison of different calculations, although not with the experimental results, is to study variation of intensity as a function of crystal thickness at a fixed angle of incidence. Curves of this type are grouped together in Figs. 11 and 12.

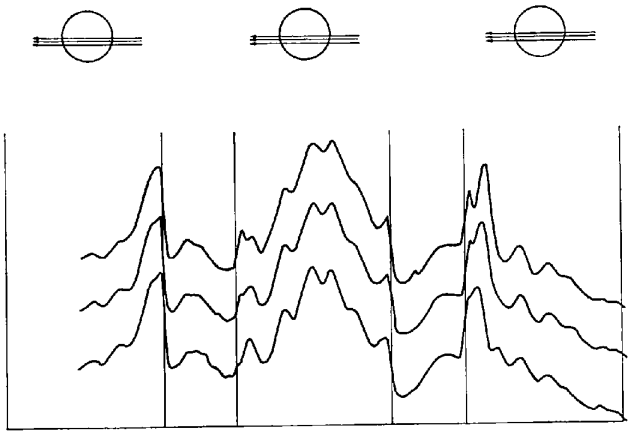

Fig. 7. Microphotometer tracings obtained from the picture shown in Fig. 6. The three tracings shown are taken as indicated by the arrows across the discs. The vertical bars in the diagram define the edges of the diffraction discs. Within each disc then, the trace measures the variation of intensity of that particular reflexion as a function of angle of incidence. The traces between the discs are a measure of the intensity of the diffuse scattering as a function of the scattering angle.

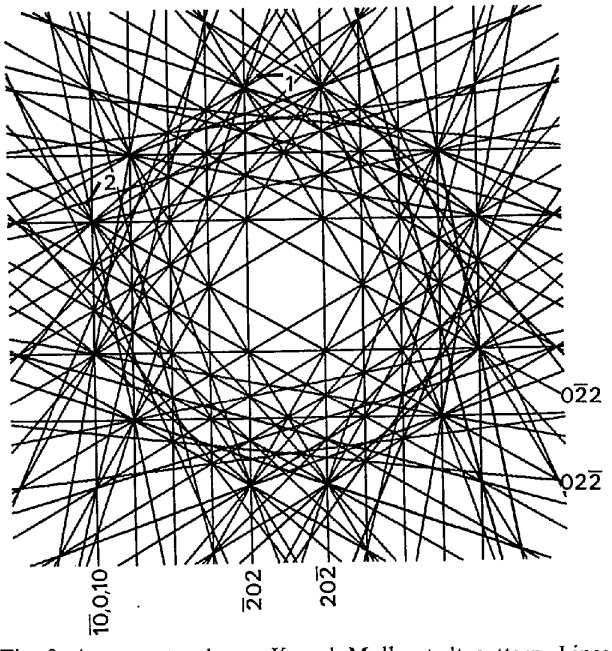

Fig. 8. A computer-drawn Kossel–Mollenstedt pattern. Lines have been drawn for the [111] zone reflexions of magnitude greater than 0·3 volt. The black bars, called 1 and 2, are then equivalent to the ranges of angle of incidence for which calculations were made.

Kossel–Mollenstedt patterns

These patterns are used to identify exactly the angles of incidence used in obtaining the diffraction patterns. In addition, computed patterns of the same angular range give some idea of the important reflexions needed in describing the diffraction patterns. In Fig. 8 is shown such a computer-drawn Kossel pattern. The pattern is made up of lines which represent the locus of angles of incidence which satisfy a particular reflexion. In this pattern, only those lines resulting from in-zone reflexions of structure amplitude greater than 0·3 volt are drawn. On the map is indicated the range of angles of incidence used in the calculations for comparison with the results shown in Fig. 7. From this map one might conclude that quite small numbers of reflexions would be sufficient to describe the experimental patterns.

In Fig. 9 is a computer-drawn Kossel pattern covering an identical range of angle to that of Fig. 8. In this case, however, the pattern includes all lines resulting from reflexions from the first nine upper layers above the [111] zone. Again, only those reflexions of structure amplitude greater than 0·3 volt are drawn. Now, if for a range of angles of incidence as represented in the Figure by the black bars are chosen, then every line intersecting the bar is a reflexion that will be satisfied. Similarly, every line in close proximity to the bar indicates a small excitation error for the corresponding reflexion. The increase in the density of lines in this second Kossel pattern is an indication of the weight of out-of-zone reflexions in dynamic calculations for gold. Both computer-drawn Kossel maps can be compared to the experimental Kossel patterns in Figs. 4 and 5. Although in the computed maps the intensities of all the lines are the same, the contrast in the experimental result is roughly comparable to the contrast produced by the densities of lines in Fig. 9.

Analog computer calculations

The analog computer was first set up to allow three-beam calculations including only the principal reflexions seen in the experimental photograph, that is the $\bar{2}20$, 000 and $2\bar{2}0$. Such a calculation by this

method requires that the value of the $\bar{4}40$ reflexion be included as it acts as a coupling factor in the calculation. The results of these calculations were displayed on a cathode ray oscilloscope and, for permanent records, on a chart recorder. The results were in the form of intensity *vs.* angle of incidence for the central beam and diffracted beams. These were recorded for a variety of thicknesses and compared with the experimental results in order to obtain an estimate of the specimen thickness. In Fig. 10(*a*) is shown the best fit obtained. This indicated that the crystal thickness was 420 ± 20 Å.

Three beams was the largest number for which rocking curve calculations could be made by the analog computer. However, by use of symmetry reductions to the problem (Johnson, 1968), the inclusion of 7 beams for calculation of variation of intensity with crystal thickness at a single angle of incidence was possible. These calculations were used to test whether the systematics approximation would be of any use in the multislice calculations. In Fig. 11, sets (*a*) and (*b*) are for 7-beam systematics and non-systematics respectively. The set of curves (*a*) were calculated using the 000, $\bar{2}20$, $2\bar{2}0$, $\bar{4}40$, $4\bar{4}0$, $\bar{6}60$, $6\bar{6}0$ reflexions. The set of curves (*b*) were calculated using the 000, $\bar{2}20$, $2\bar{2}0$, $\bar{4}22$, $2\bar{4}2$, $\bar{6}24$, $2\bar{6}4$ reflexions. Comparison of the relative intensities of the $\bar{4}40$, $4\bar{4}0$ and $\bar{4}22$, $2\bar{4}2$ reflexions indicated that for the angle of incidence used more intensity was absorbed into the $\bar{4}22$, $2\bar{4}2$ reflexions than into the $\bar{4}40$, $4\bar{4}0$ reflexions. Thus it was felt that the systematics approximation would not be appropriate for more detailed calculations. The curves in Fig. 11, sets (*a*) and (*b*) of the central beam and $\bar{2}20$ reflexions, show a change only of curve shape from sinusoidal form in the systematics case to a non-sinusoidal form in the non-systematics case. The angle of incidence for these calculations corresponds to the centre of the rocking curve of the central beam in Fig. 10(*a*). This is the case when the excitation errors of the $\bar{2}20$ and $2\bar{2}0$ reflexions are exactly equal.

Multislice calculations

Initially, for calculations involving only zone reflexions, a phase grating was calculated using Hartree–

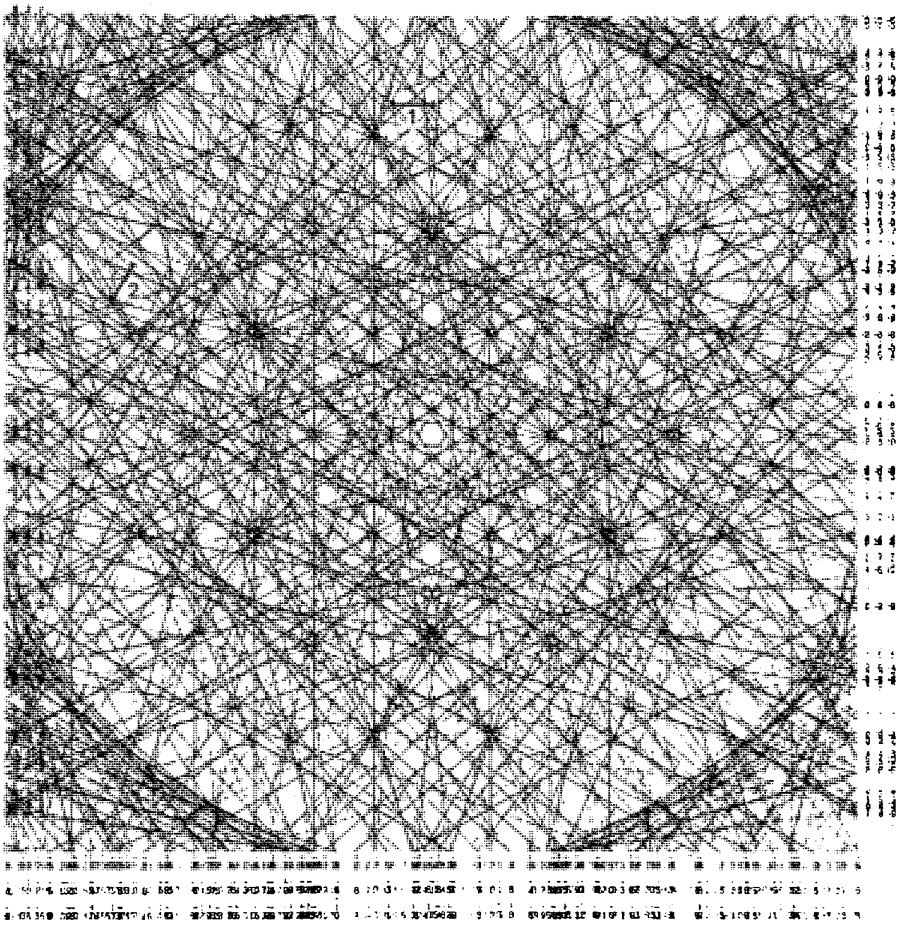

Fig. 9. A computer-drawn Kossel–Mollenstedt pattern. Lines have been drawn for reflexions of magnitude greater than 0·3 volt. The same angular range has been covered as in Fig. 8. In this case, however, reflexions from the first nine upper layers above the [111] zone have been included.

Fock–Slater form factors for gold from *International Tables for X-ray Crystallography* (1962). The phase grating included a total of 611 reflexions centred about the [111] zone axis. The slice thickness was found to be satisfactory if less than 3·5 Å. It was chosen to be 2·36 Å for convenience of comparison with upper layer-line calculations. Using 37 reflexions from this phase grating, multislice calculations were made to a thickness of 500 Å. At this thickness, the sum of intensities in the diffracted beams was 87% of the initial intensity. The calculations were quite rapid, taking one minute per angle of incidence.

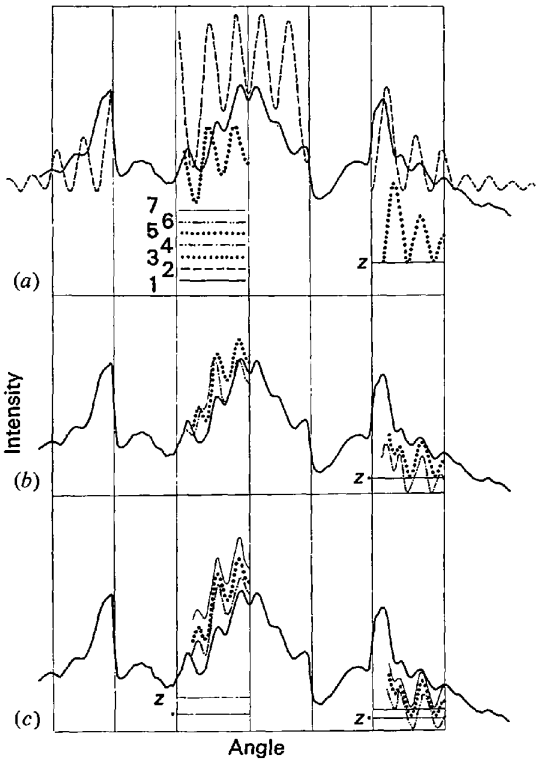

Fig. 10. Calculated rocking curves compared with measured rocking curves. (*a*) Comparison of analog computer calculations with 37-beam multislice calculations and with experiment. (*b*) Comparison of 129-beam multislice calculations including upper layer line effects with experiment. Curve 5 was made for the range of angles shown in Fig. 8 at bar number 2. Curve 4 was made for the range of angles shown in Fig. 8 at bar number 1. (*c*) Comparison of 129-beam multislice calculations for three thicknesses separated by one face-centred cubic unit cell diagonal (7·08 Å), illustrating best fit for a thickness of 417·7 Å. Identification of curves: (1) Experimental microphotometer traces. (2) 3-beam analog computer calculation for a thickness of 420 Å. (3) 37-beam multislice calculation, thickness 420 Å. Zone reflexions only. (4) 129-beam upper layer-line calculation, thickness 417·7 Å. Angular range is that indicated in position 1, Fig. 8. (5) 129-beam upper layer-line calculation, thickness 417·7 Å. Angular range is that indicated in position 2, Fig. 8. (6) 129-beam upper layer-line calculation, thickness 410·6 Å. (7) 129-beam upper layer-line calculation, thickness 424·8 Å. The lines marked with *z* indicate the amount by which the zero of the associated calculated curve has been offset.

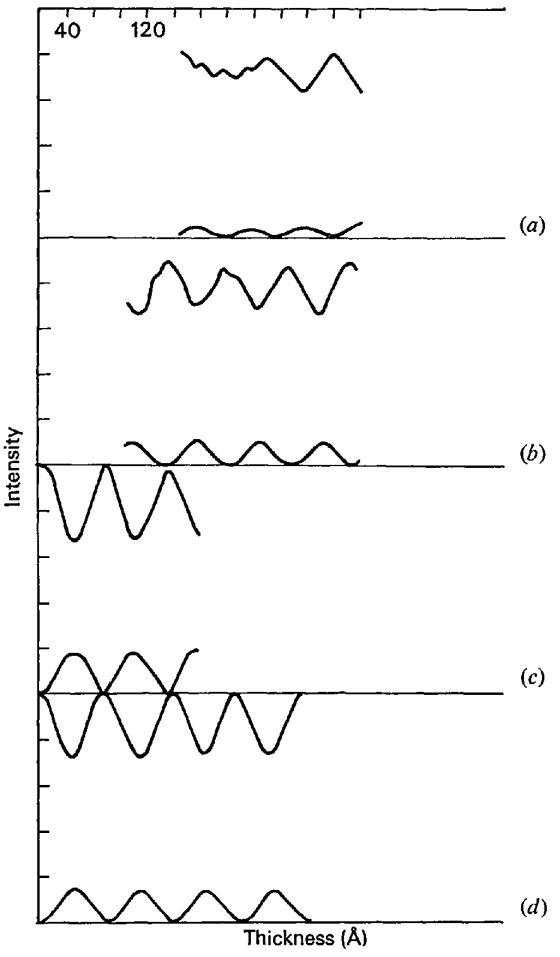

Fig. 11. Calculated curves of intensity as a function of crystal thickness. Angle of incidence is that corresponding to the centre point in the rocking curves for the 000 reflexion in Fig. 10. (*a*) Analog computer 7-beam systematics approximation. (*b*) Analog computer 7-beam non-systematics case. (*c*) Multislice calculation for 37 beams and slice thickness of 2·36 Å. (*d*) Multislice calculation for 37 beams and slice thickness of 7·08 Å.

For the case of exactly equal excitation errors for the $\bar{2}20$ and $2\bar{2}0$ reflexions, curves of intensity *vs.* thickness were recorded [Fig. 11(*c*)]. These curves are compared with the analog computer 7-beam calculations. The period of oscillation in the curves is only approximately comparable and the detailed shapes are different. In Fig. 11(*d*) is shown the effect of too great a slice thickness, *i.e.*, 7·08 Å. The extra turning points in these curves are a result of too great a slice thickness.

Curves of intensity *vs.* angle of incidence for a range of thicknesses about 420 Å were calculated. In Fig. 10(*a*) is shown the best fit of these curves with the experimental rocking curves. The fit with experiment is quite poor as none of the turning points in the curves coincide. It can be seen that there has been a small change in the curve profiles between the three-

beam analog computer calculations and the 37-beam multislice calculations.

The poor fit with experiment necessitated calculations with better representation of out-of-zone effects. A phase grating was constructed from a single atom layer 2·36 Å thick having 611 reflexions of which 211 reflexions are in the zone. Identical form factors were used as for the zone-only calculations. In terms of face-centred cubic indices, the phase grating covers as far out in the [111] zone as the $\bar{1}4,14,0$ reflexion. Multislice calculations were then made using 129 beams, 43 beams in the [111] zone, to a crystal thickness of 500 Å. The sum of intensities in the diffracted beams was then only 75% of the initial intensity. This sum of intensity is considered to be only marginally satisfactory, however since the calculations took eight minutes per angle of incidence, the number of beams was not increased.

Typical behaviour of out-of-zone reflexions in these calculations can be seen in Fig. 12. In this Figure is shown the variations of intensity with thickness of the $\bar{1}11$ reflexion for the case of the $\bar{2}20$ reflexion exactly satisfied. For numbers of slices not divisible by three the intensity of this reflexion is as high as 4 to 5×10^{-3} of the incident intensity. At every third slice, however this intensity falls to values less than 1×10^{-3} of the incident intensity. The remaining intensity in this out-of-zone reflexion, in the case of integral numbers of unit cells, was sufficient to give some hope of detection in the convergent beam diffraction camera. Many long-exposure pictures were taken, of which quite a few were spoilt by ion damage of the crystal. Of the few pictures from undamaged crystals it was found that the angles at which the upper layer-line reflexions occurred coincided with maxima in the thermal diffuse intensity distributions (Fig. 13) for the crystals examined, all being about 350 to 450 Å in thickness. In conventional parallel beam diffraction patterns taken from these foils, the extra points can be seen (Fig. 14), however these average over a larger area of the gold foil and will contain contributions due to stacking faults in the crystal. Better pictures of out-of-zone reflexions from [111] gold foils were observed by Sanders & Allpress (unpublished) by selected area diffraction from very thin foils, about 20 to 40 Å thick.

In Fig. 10(*c*) are shown curves of intensity *vs.* angle of incidence for three thicknesses compared with the experimental results. The thickness intervals correspond to one unit cell of gold. The fit in the diffracted beam $\bar{2}20$ is the best for 417·7 Å crystal thickness. It can be seen that the degree of fit has improved a great deal over the zone-only calculation. No attempt has been made to subtract the diffuse background from the experimental microphotometer traces so the degree of fit is judged by the alignment of turning points of the calculated and experimental curves. The fit of the central beam breaks down towards the edge of the convergent beam disc.

A minimal angular range was selected for these calculations because of computer time limitations. Only eleven points were sampled across the range, the computation time being eight minutes per point.

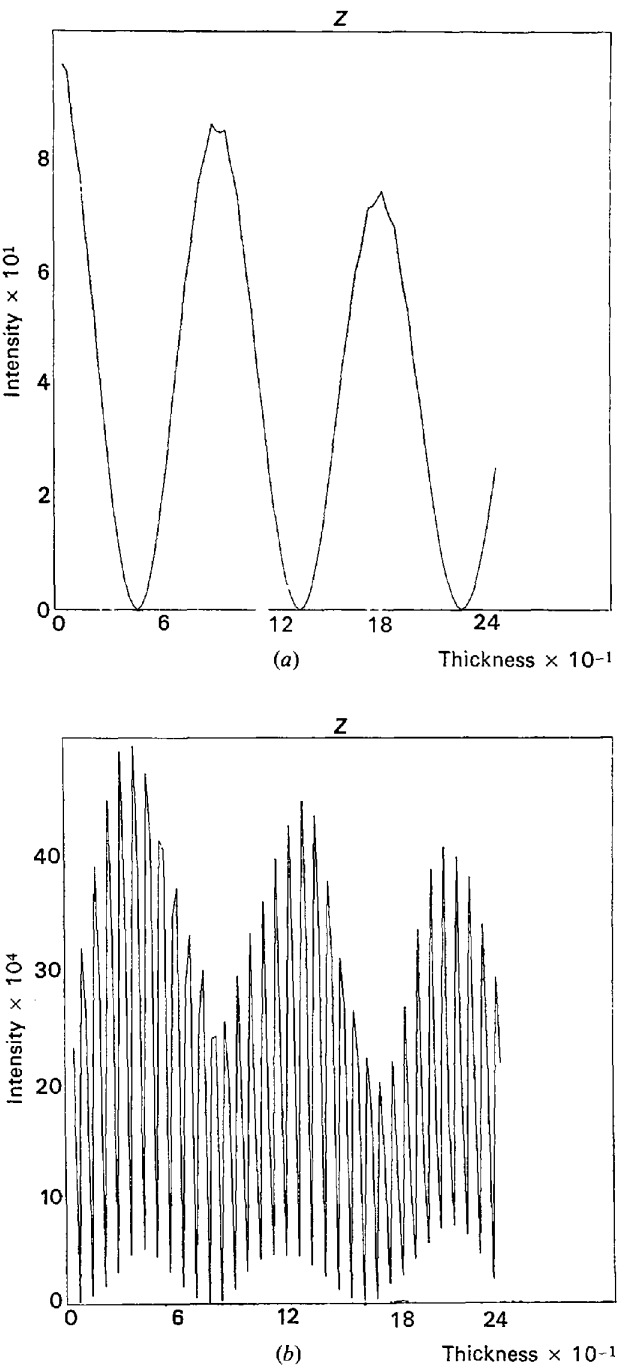

Fig. 12. Variation of intensity as a function of crystal thickness for the case of the $2\bar{2}0$ reflexion satisfied. (*a*) 000 reflexion. (*b*) $\bar{1}11$ reflexion. The intervals of calculation corresponds to one atom layer thickness on the crystal.

Symmetry

In Fig. 8 two ranges of angles of incidence, separated by 60 degrees, are indicated. For the [111] zone, which has hexagonal symmetry, these two ranges are equivalent. As a check for the zone-only calculations, both ranges were used and the results were identical.

When effects out of the [111] zone are included, the symmetry becomes trigonal, that is, the symmetry of a cube viewed down the body diagonal rather than that of a projected cube. Thus when calculations were made over both ranges, small differences in the intensity *vs.* angle of incidence curves were observed [Fig. 10(*b*)]. The differences are sufficiently great to allow identification of the experimental results with respect to one azimuth than the other.

Conclusions

It must be emphasized that these calculations have been purely elastic, that is, no absorption parameters have been included. Only one thermal parameter and one set of form factors have been used. The set of Hartree–Fock–Slater form factors used were obtained from *International Tables for X-ray Crystallography* (1962) and differ by only 1 % from more recent values published (Doyle & Turner, 1967). Nonetheless, reasonable fit with experiment has been obtained. The poor fit of the central beam near the edge of the convergent-beam disc indicates that some refinement of the form factor for gold is necessary. At this stage it is not known whether the fit is improved by using the form factors of Doyle & Turner (1967).

It appears that none of the approximations used in measurement of form factors for light atoms to 1 % are applicable to gold; that is, the systematics approximation or the two-dimensional (zone-only) approximation.

The calculations show that it is necessary to include out-of-zone information in order to describe the intensities of diffracted beams from a gold single crystal. For the particular range of angles chosen the lack of agreement between a zone-only calculation and experiment is quite large. The lack of agreement is illustrated by the correspondence of a maximum in the calculated curve for the diffracted beam $2\bar{2}0$ with a minimum in the experimental curve, Fig. 10(*a*), curve number 3, the first maximum in the calculated curve for the $2\bar{2}0$ reflexion. The inclusion of out-of-zone reflexions has removed this disagreement with experiment. Phenomenological absorption parameters used in conjunction with a zone-reflexions-only calculation could not be used to represent out-of-zone reflexions because they could not supply the additional dynamical coupling paths that exist by way of the out-of-zone reflexions. Thus the absorption parameters would exhibit the difficulties inherent in using such parameters to represent weak-beam effects. That is each absorption parameter would be found to have variation in magnitude with angle of incidence. This variation may not be immediately apparent by measurements which average over a range of angles of incidence of the order of three to four minutes of arc or greater. It is felt that the next step to higher precision in calculation of diffracted beam intensities for gold would be the inclusion of phenomenological absorption parameters in addition to out-of-zone reflexions.

For quick estimation of coarse features in electron diffraction from gold, only a few beams in some orientations seem to be necessary; for example, the quick estimation of crystal thickness to low accuracy.

For calculations near the zone axis in gold, within 0·01 radian, even with 127 reflexions, at a thickness of 500 Å the sum of intensities in the beams was only 0·2 electrons. Thus it seems that for such a heavy atom, even with a small unit cell, calculations close to a zone axis would be very time consuming, since many more than 127 reflexions would need to be included.

The author wishes to thank Dr A. W. S. Johnson for his help with computing methods, and Dr J. V. Sanders and J. Allpress for showing to him point diffraction patterns obtained from [111] gold foils of thickness of the order of 25 Å. The author is indebted to Mr A. F. Moodie for many helpful discussions on the theory.

References

COCKAYNE, D. J. H., GOODMAN, P., MILLS, J. C. & MOODIE, A. F. (1967). *Rev. Sci. Instrum.* **38**, 1097.
COWLEY, J. M. & MOODIE, A. F. (1957). *Acta Cryst.* **16**, 699.
DOYLE, P. A. & TURNER, P. S. (1967). *Acta Cryst.* A**24**, 390.
FISHER, P. M. J. (1968). *Japan J. Appl. Phys.* **7**, 191.
GOODMAN, P. & LEHMPFUHL, G. (1967). *Acta Cryst.* **22**, 14.
HOWIE, A. & WHELAN, M. J. (1962). *Proceedings of European Regional Conference on Electron Microscopy*, Delft. p. 181.
International Tables for X-ray Crystallography (1962). Vol. III. Birmingham: Kynoch Press.
JOHNSON, A. W. S. (1968). *Acta Cryst.* A**24**, 534.
MOODIE, A. F. (1965). *International Conference on Electron Diffraction and Crystal Defects*, Melbourne.
NIEHRS, H. (1959). *Z. Phys.* **156**, 446.
STURKEY, L. (1962). *Proc. Phys. Soc.* **80**, 321.